Received: 14 March 2022 | Revised: 20 June 2022 | Accepted: 21 June 2022

DOI: 10.1111/mmi.14956

RESEARCH ARTICLE

WILEY

Histidine auxotroph mutant is defective for cell separation and allows the identification of crucial factors for cell division in *Brucella abortus*

Agnès Roba | Elodie Carlier | Pierre Godessart | Cerine Naili | Xavier De Bolle

Research Unit in Biology of Microorganisms, Narilis, University of Namur, Namur, Belgium

Correspondence
Xavier De Bolle, Research Unit in Biology of Microorganisms, Narilis, University of Namur, Namur B-5000, Belgium
Email: xavier.debolle@unamur.be

Funding information
Federation Wallonie-Bruxelles, Grant/Award Number: ARC 17/22-087; Fonds De La Recherche Scientifique - FNRS, Grant/Award Number: T.0058.20 and T.0060.15

Abstract

The pathogenic bacterium *Brucella abortus* invades and multiplies inside host cells. To grow inside host cells, *B. abortus* requires a functional histidine biosynthesis pathway. Here, we show that a *B. abortus* histidine auxotroph mutant also displays an unexpected chaining phenotype. The intensity of this phenotype varies according to the culture medium and is exacerbated inside host cells. Chains of bacteria consist of contiguous peptidoglycan, and likely result from the defective cleavage of peptidoglycan at septa. Genetic suppression of the chaining phenotype unearthed two essential genes with a role in *B. abortus* cell division: *dipM* and *cdlP*. Loss of function of *dipM* and *cdlP* generates swelling at the division site. While DipM is strictly localized at the division site, CdlP is localized at the growth pole and the division site. Altogether, the unexpected chaining phenotype of a *hisB* mutant allowed the discovery of new crucial actors in cell division in *B. abortus*.

KEYWORDS
Brucella, cell division, peptidoglycan

1 | INTRODUCTION

The alphaproteobacterial order Rhizobiales comprise a great diversity of bacteria in terms of shape and lifestyle. They include plant symbionts (*Rhizobium*) and pathogens (*Agrobacterium*), free-living bacteria (*Ochrobactrum*), and animal pathogens (*Bartonella*, *Brucella*) (Batut et al., 2004). Bacteria from the genus *Brucella* are able to infect a broad range of vertebrates and are responsible for a worldwide zoonosis known as brucellosis (Whatmore & Foster, 2021). *Brucella abortus* is a Gram negative facultative intracellular pathogen which causes sterility and abortion in cattle and a debilitating febrile illness sometimes referred to as Malta fever in humans (Pappas et al., 2006). This bacterium displays some characteristics of the alphaproteobacteria, such as cell cycle regulation by CtrA (Francis et al., 2017), and unipolar growth which was also observed in other Rhizobiales such as *Agrobacterium tumefaciens* and *Sinorhizobium meliloti* (Brown et al., 2012). Unipolar growth is characterized by two main steps along the cell cycle: incorporation of new cell envelope components at the new pole and cell division. Many genes of *B. abortus* have been predicted to be involved in cell division by homology with *Escherichia coli* or *Caulobacter crescentus* (Sternon et al., 2018), however their function has not been characterized so far.

Brucella abortus can invade, and survive and proliferate inside host cells including macrophages, where it resides in a membrane-bound compartment known as the *Brucella*-containing vacuole (BCV). During the first hours of infection, *B. abortus* initially traffics through an acidic vacuole derived from the endocytic pathway (Starr et al., 2008). Then, it manages to reach the endoplasmic reticulum, inside which it will proliferate (Celli et al., 2003). Unlike many other intracellular bacteria that have coevolved for a long time with their eukaryotic host, *B. abortus* has not undergone a major

genome reduction and retains broad biosynthetic abilities (Batut et al., 2004). Notably, *B. abortus* is prototrophic for all 20 amino acids. Recently, the ability of *B. abortus* to survive and grow inside the infection model RAW 264.7 macrophages has been investigated by Tn-seq (Sternon et al., 2018). Genes required during infection of this model host cell were identified, and the histidine biosynthesis pathway genes, including *hisB*, were predicted to be essential for intracellular proliferation.

To investigate the importance of histidine biosynthesis for *B. abortus* during infection, we characterized the ability of auxotrophic *hisB* mutants to proliferate inside HeLa cells. Surprisingly, besides showing a decreased intracellular proliferation, loss of function *hisB* mutants exhibited a chaining morphology inside HeLa cells. Characterization of this chaining morphology revealed that it was due to a cell separation defect, originating from incomplete PG cleavage during late division. Overexpression of two lipoproteins with putative role in cell division, a DipM endopeptidase homolog and a protease that was renamed CdlP suppressed the chaining phenotype of the *hisB* mutant. Localization and depletion of these two essential factors confirmed their role in cell division in *B. abortus*.

2 | RESULTS

2.1 | The auxotrophic mutants Δ*hisB* and $hisB_{E17Q}$ replicate less efficiently inside host cells

HisB is the sixth enzyme involved in the histidine biosynthesis pathway (Figure S1a). It is the first enzyme of the pathway to be specifically dedicated to histidine biosynthesis, as the five first enzymes also contribute to the generation of 5-aminoimidazole-4-carboxamide ribonucleotide (AICAR), a metabolic intermediate of the purine biosynthesis pathway (Figure S1a). HisB is a dehydratase that generates imidazole-acetol-phosphate from imidazole glycerol phosphate (IGP). In frame deletion of *hisB* makes *B. abortus* auxotrophic for histidine since it does not affect growth in Plommet erythritol (PE) minimal medium supplemented with 1 mM histidine, but it renders the bacterium unable to grow in PE without histidine (Figure S1b). The growth defect of this auxotrophic mutant can be fully rescued by *in trans* expression of *hisB* (Figure S1b). Using site-directed mutagenesis, we produced a catalytically inactive mutant of *B. abortus hisB*, $hisB_{E17Q}$, by replacing glutamate 17 in HisB with a glutamine (Figure S1b). This point mutation phenocopies *hisB* deletion in terms of growth (Figure S1b). We then evaluated the ability of these mutants and the complemented Δ*hisB* mutant to replicate inside HeLa cells. The Δ*hisB* and $hisB_{E17Q}$ mutations strongly affect intracellular proliferation at 24 and 48 h post infection (Figure 1). This replication defect inside HeLa cells can be rescued either by genetic complementation, or by the addition of 10 mM histidine in the HeLa cell culture medium. These results suggest that *B. abortus* relies on de novo histidine biosynthesis for intracellular replication.

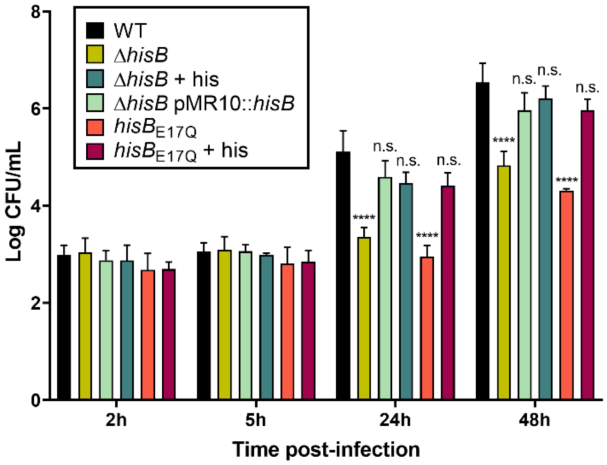

FIGURE 1 Functional HisB is required for *B. abortus* intracellular replication. Intracellular replication of WT, deletion mutant Δ*hisB*, catalytically dead mutant $hisB_{E17Q}$ and the complemented Δ*hisB* mutant were assessed by enumerating colony-forming units (CFU) after 2, 5, 24, and 48 h post infection of HeLa cells. When indicated, 10 mM histidine was added in the medium at the beginning of the infection. Data represent mean ± SD and were compiled from three independent replicates. Statistical significance between results for a given strain and those for the WT was determined by two-way ANOVA followed by Dunnett's multiple comparison test (n.s., not significant; $^{****}p < 0.0001$).

2.2 | The *hisB* mutants display chaining morphology inside HeLa cells

Very surprisingly, besides being attenuated inside HeLa cells, the Δ*hisB* and $hisB_{E17Q}$ mutants also show a striking chaining morphology at 24 h post infection (Figure 2). The addition of 10 mM histidine to the HeLa cell culture medium restores both intracellular replication and normal morphology of the mutants. This finding supports the idea that histidine is not only required for intracellular proliferation of the brucellae but also for their normal morphology within the intracellular environment. We then checked whether the chains were formed inside the host cells, or formed prior to contact with host cells and then internalized as such. Indeed, even though a small proportion of chains is found in rich medium, the entry of chaining bacteria could somehow be favored. To test this possibility, before infection, bacteria were stained with eFluor (Cell Proliferation Dye eFluor™ 670), a dye which covalently binds to the bacterial surface and was previously used to show unipolar growth in *B. abortus* (Vassen et al., 2019). After bacteria were stained with eFluor, they were washed and then incubated with HeLa cells. At 4 and 24 h post infection, cells were fixed and stained with anti-*Brucella* (S-LPS) antibodies to detect all intracellular bacteria (Figure S2). Therefore, bacteria that were immunolabeled but were negative for eFluor have been newly generated inside host cells. At 4 h post infection, intracellular *Brucella* are mostly isolated and positive for eFluor, regardless of the genotype. At 24 h post infection, WT as well as *hisB* mutant strains appeared to derive from only one or two "mother" cells stained with eFluor. This indicates that *hisB* mutant

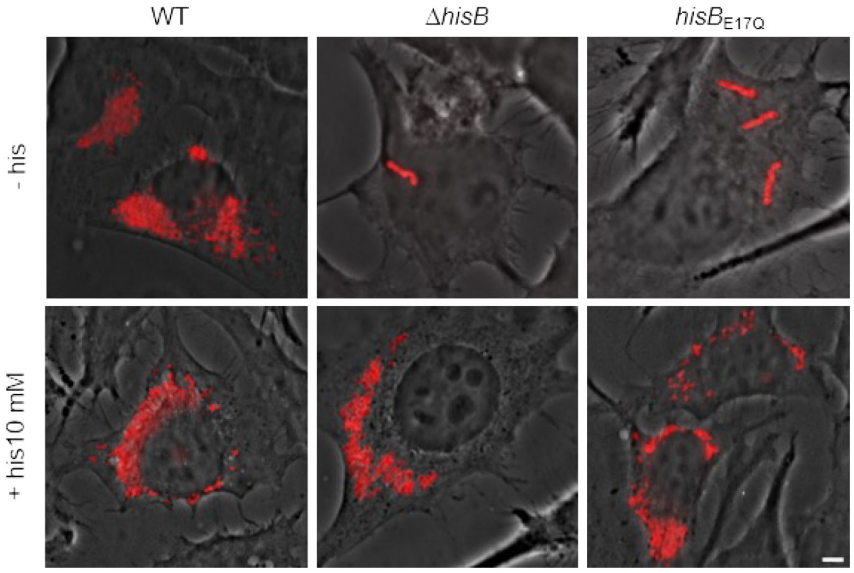

FIGURE 2 Morphology of *B. abortus hisB* deletion and catalytic mutants during infection of HeLa cells. Immunofluorescence microscopy of HeLa cells infected for 24 h with WT, Δ*hisB* or *hisB*$_{E17Q}$ strains. Phase contrast images were merged with anti-*Brucella* (S-LPS) staining (red) to detect intracellular bacteria. Chaining morphology was observed in 97.5% ($n = 80$) and 98.9% ($n = 93$) of infected cells with Δ*hisB* and *hisB*$_{E17Q}$, respectively. This percentage falls down to 20% ($n = 73$) and 8.4% ($n = 60$) when histidine is added to the medium during the infection. (Scale bar: 5 μm).

chains are indeed formed by the brucellae replicating after entry into HeLa cells, likely due to a problem of cell division.

2.3 | Chaining phenotype intensity varies with the culture medium in vitro

When the Δ*hisB* strain was cultured in TSB, the usual rich medium used for *B. abortus*, a very low percentage of chaining bacteria was observed under the microscope (Figure 3a,b). However, the proportion of chains increased when the bacteria were grown in Heart Infusion broth (HI), another rich medium, or in Gerhardt's minimal medium supplemented with 0.1% casamino acids (GCA) (Figure 3c,d). The nature of the culture media strongly affected the morphology of Δ*hisB* mutant, but not the morphology of the WT *B. abortus*. Although GCA and HI are very different media, they both generated chaining phenotypes but the length distribution is very different between these two media. Surprisingly, we found out that the *B. abortus* parental strain was also displaying chains in HI, when exposed to relatively high amounts of zinc (1 mM). This phenotype was quantified by measuring the length of a high number of bacteria ($326 < N < 890$) that were exposed or not to zinc. The distribution of lengths of the parental strain exposed to zinc is significantly higher compared with unexposed bacteria and tends to resemble the one of the Δ*hisB* mutant. Interestingly, the presence of the metal chelator EDTA strikingly prevents chain formation in the Δ*hisB* mutant (Figure S3). The ability to reproduce the chaining phenotype in culture in specific conditions suggests that it is metal-dependent and offers the opportunity to investigate its generation.

2.4 | Chaining is generated by uncleaved peptidoglycan at cell division sites

Typically, chaining morphology is due to a defect of cell separation, the last step of cell division (Heidrich et al., 2002; Uehara et al., 2009). Division defects in bacteria belonging to the order Rhizobiales lead to many different aberrant morphologies, such as branching, elongated, and spherical cells (Latch & Margolin, 1997). Since *B. abortus* is growing in a unipolar fashion like all other Rhizobiales investigated so far (Brown et al., 2012), we investigated how new cell wall material was inserted inside chaining bacteria. First, bacteria were stained with eFluor, then they were washed and then allowed to grow for 5 h in HI medium without eFluor, thus newly generated envelope appears as unstained. Then, we performed a short pulse labeling with the fluorescent D-amino acid HADA to highlight newly inserted peptidoglycan (PG) (Kuru et al., 2012) (Figure S4). Constriction sites and growing poles appear in blue (HADA), whereas older envelopes, typically in "mother" cells are labeled in far red (eFluor). The combination of these two dyes shows us that new cell wall material is still incorporated in a unipolar fashion inside the chains. The eFluor labeled either a terminal pole of the chains or an internal segment within the chains (Figure S4). Strikingly, the vast majority of contacts between cells within the chains are also labeled with HADA (Figure S4), which could be due to either incomplete division or closely associated new (growing) poles. This raised two possible hypotheses for the generation of chains, either bacteria are still connected by continuous PG, which is not completely split at division sites, or PG splitting is complete and bacteria remain connected by their outer membrane. As it is possible to highlight chains with connected PG by the imaging of sacculi (Yakhnina & Bernhardt, 2020), we purified sacculi of the different strains and checked if they are still forming chains. We checked that these purified sacculi bind wheat germ agglutinin and a monoclonal antibody recognizing *Brucella* PG, but not a monoclonal antibody directed against lipopolysaccharide, which indicates that outer membrane has been removed (Figure S5). When Δ*hisB* or *hisB*$_{E17Q}$ mutants were grown in HI, in the conditions where chaining phenotype is easily observable, the sacculi obtained are still forming chains, which confirms that these chains of bacteria are made of connected peptidoglycan. Accordingly, late division steps that normally lead to final

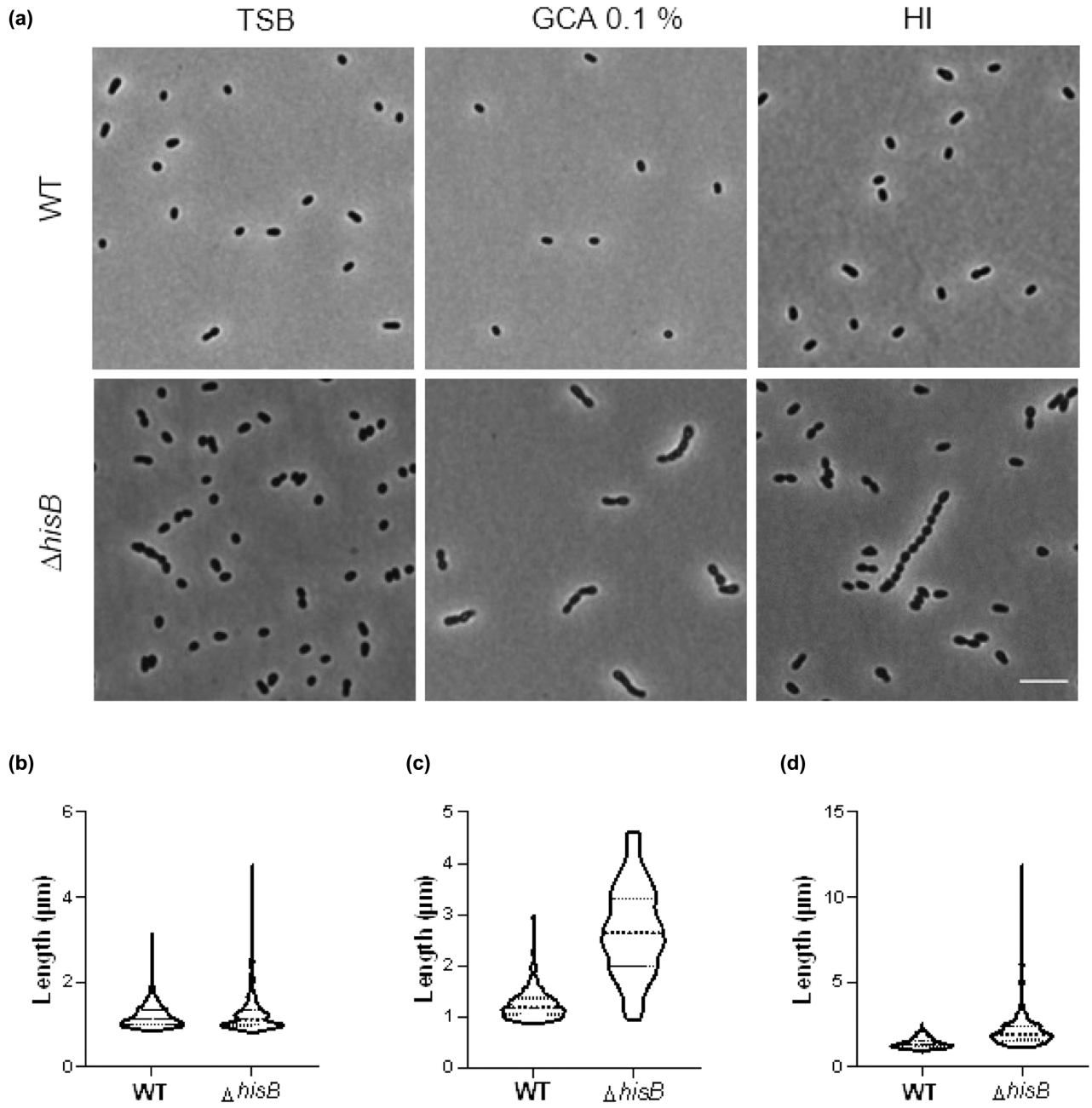

FIGURE 3 Cell morphology of the *B. abortus* Δ*hisB* mutant is dependent on growth conditions. (a) Morphology of WT and an isogenic Δ*hisB* mutant grown in rich medium (TSB), minimal medium (Gerhardt + 0.1% Casamino Acids), and another rich medium (HI). Scale bar: 5 µm. Bottom panels indicate cell length distribution ($100 < n < 450$) depending on corresponding growth conditions (b–d). The length axis was adapted to chain length in each culture condition.

separation of the cells seem to be compromised in a strain with a deleted or catalytically dead *hisB*.

2.5 | Suppression of the *hisB* chaining phenotype

Considering the lack of knowledge regarding the repertoire of enzymes digesting PG in *B. abortus*, we first performed a bioinformatic analysis to identify and classify putative PG hydrolyzing enzymes encoded by the *B. abortus* genome. Predicted PG hydrolases were identified based on homology with *A. tumefaciens* and *Caulobacter crescentus* PG hydrolases and thanks to the "HyPe" tool, a software designed to identify PG hydrolases (Sharma et al., 2016). We compared the list of genes obtained with two sets of data acquired previously, the first being predicted essential identified by Tn-seq data analysis (Sternon et al., 2018) and the second being direct target genes of the cell division regulator CtrA identified by ChIP-seq analysis (Francis et al., 2017) (Table S1). Only two of these genes were potentially essential (BAB1_0907 and BAB1_1773), while three others (including BAB1_0931) were considered "low fitness,"

suggesting that loss of function of the gene could be tolerated but would compromise growth and/or survival. An obvious candidate to be an important division factor in *B. abortus* is BAB1_0907, the homolog of DipM in *C. crescentus* since this gene is proposed to be both essential and regulated by CtrA (BAB1_0907 was thus renamed *dipM*). We decided to check whether overexpression of this *B. abortus dipM* gene would compensate the chaining phenotype of Δ*hisB*, by integrating $dipM_{Ba}$ on a medium-copy plasmid. We also tested the overexpression of the essential LysM domain-containing protease BAB1_1773 and the only periplasmic amidase BAB1_0931, which is almost essential. Overexpression of *dipM* and BAB1_1773 but not BAB1_0931 significantly reduces chaining, as indicated by cell length measurements (Figure 4). The data obtained with *dipM* overexpression are consistent with a PG separation defect in the chains, and they suggest that BAB1_1773, a conserved lipoprotein of unknown function displaying a LysM domain and a predicted M48 protease domain, could also be involved in cell division. BAB1_1773 was thus renamed *cdlP* (**c**ell **d**ivision **L**ysM-containing **p**rotease).

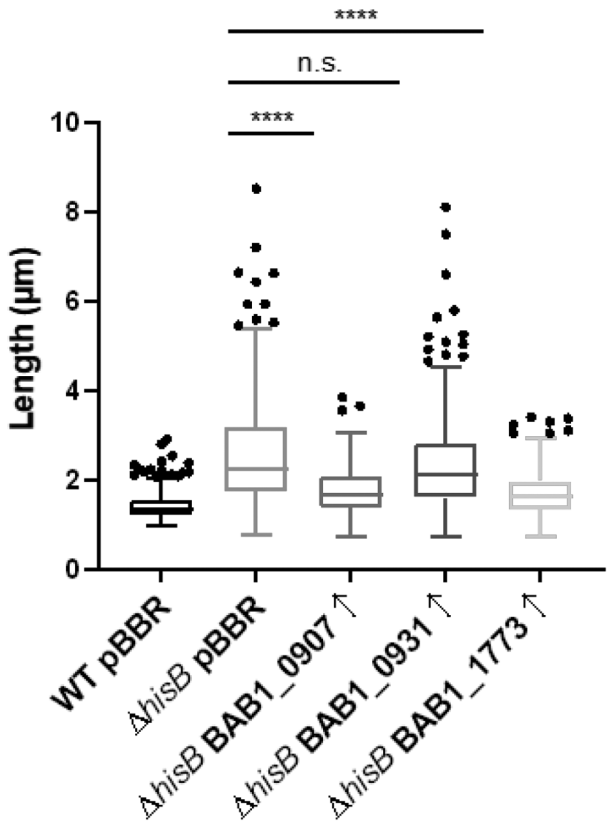

FIGURE 4 Length distribution of WT (n = 314), Δ*hisB* (n = 296), and Δ*hisB* strains overexpressing BAB1_0907 (n = 339), BAB1_0931 (n = 263), and BAB1_1773 (n = 290). All strains were grown in HI with chloramphenicol, with the WT and Δ*hisB* carrying an empty pBBR1 vector, whereas overexpression strains carry a pBBR1 vector with the corresponding genes. Dots represent outlier values according to Tukey's rule in GraphPad Prism. Distributions were analyzed using Dunn's multiple comparison tests after Kruskal–Wallis. ****$p < 0.0001$.

2.6 | DipM and CdlP are involved in cell divison

DipM and CdlP are both predicted to contain a PG-binding domain called LysM (Figure 5a,d). Since it is expected that cell division proteins will be localized at constriction sites, we fused DipM and CdlP with the fluorescent protein mNeonGreen (mNG). Both fusion proteins were found to localize at cell septa, in WT as well as the Δ*hisB* mutant strain, further supporting the role of these proteins in cell division (Figure 5b,e, Figure S6). DipM localization is restricted at midcell in dividing bacteria (Figure 5b), whereas CdlP appears to be localized both at septa and at the growing pole (Figure 5e, Figure S7). As both *dipM* and *cdlP* are predicted to be essential, we used a anhydrotetracycline (AHTC)-inducible CRISPR-intereference (CRISPRi) system to deplete the corresponding gene products. Depletion of DipM leads to the generation of large bulges at midcell, very similar to what was observed when *B. abortus* is treated with the antibiotics aztreonam and cephalexin which target the division machinery in *E. coli* (Figure 5c) (Eberhardt et al., 2003). Depletion of CdlP also generates bulges at midcell, although smaller than when DipM is depleted (Figure 5f). HADA staining highlights the abnormally large midcell bands observed in CdlP depleted cells, in comparison with a strain expressing CdlP at normal levels (Figure 5f).

3 | DISCUSSION

Division defects in Rhizobiales usually lead to very diversified morphologies, such as branches, spheres, bulges, or the generation of buds (Francis et al., 2017; Latch & Margolin, 1997). Here, we identified a characteristic chaining phenotype related to cell division, although originating from an a priori unrelated function, i.e. histidine biosynthesis. This unusual morphology phenotype allowed us to identify essential actors of cell division, DipM and CdlP, which have not been characterized yet in *B. abortus*.

In this work, we propose that the chaining phenotype is due to incompletely digested PG at septa in *hisB* defective cells. On the one hand, PG sacculi extracted from Δ*hisB* mutant conserved the chaining morphology (Figure S5). On the other hand, overexpression of two essential proteins predicted to be PG-associated suppressed the chaining phenotype. We could also show by fusing DipM and CdlP with mNG that both enzymes are localized at the constriction site in dividing cells, both in the WT and Δ*hisB* mutant (Figure S6), consistent with the role of these two proteins in cell separation in *B. abortus*.

DipM is a M23 family endopeptidase, a family of enzymes cleaving bonds between amino acids of the stem peptide of the PG. DipM was shown to be involved in PG remodeling during cell division in *C. crescentus* (Moll et al., 2010). In distant organisms such as cyanobacteria, DipM was also found to be involved in cell separation, and is even conserved in chloroplasts of some algae, where it also allows division through PG digestion (Miyagishima et al., 2014). More recently, it has been shown that the homolog of DipM in *Agrobacterium tumefaciens* ($DipM_{At}$) is likely to have

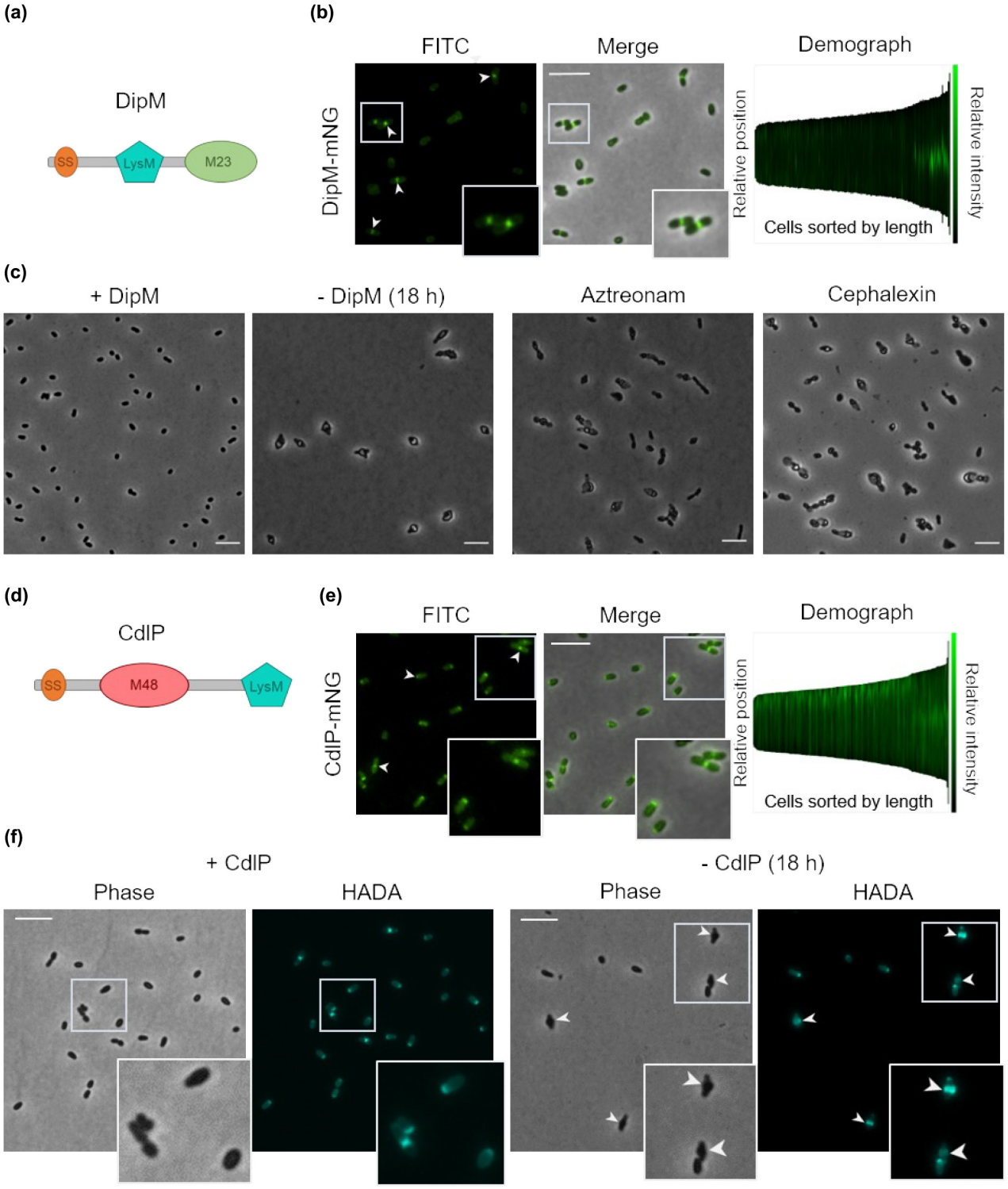

FIGURE 5 DipM and CdlP are involved in cell division in *B. abortus*. Schematic of the domain organization of DipM (a) and CdlP (d). Both comprise a LysM domain and a predicted lipoprotein signal sequence (SS). Overnight cultures of *B. abortus* strains bearing the DipM-mNG (b) or CdlP-mNG (e) fusion were imaged on agarose pads by phase-contrast and fluorescence microscopy. Arrows show midcell and/or polar localization. Demographic representation of mNG localization was obtained after bacteria were sorted by cell length and show midcell localization of DipM in dividing cells ($N = 246$) (b) and polar and midcell localization of CdlP ($N = 216$) (e). (c) Phase-contrast images of DipM-depleted cells after 18 h of growth in the presence of anhydrotetracycline (AHTC) (left panels), or after 18 h of growth in the presence of 100 μg/ml of aztreonam and cephalexin (right panels). (f) Phase-contrast and fluorescence images of CdlP-depleted cells after 18 h of growth in the presence of AHTC, and after HADA labeling. Arrows show bulges at midcell. Scale bars: 5 μm.

broader functions than just the direct hydrolysis of PG to promote cell separation (Figueroa-Cuilan et al., 2021). Indeed, catalytic residues of the active site of $DipM_{At}$ are not conserved, similarly to their homologs in *E. coli*, EnvC and NlpD. In *E. coli*, these two factors do not have endopeptidase activity on their own but instead activate the amidases (AmiA, AmiB and AmiC) that are responsible for PG splitting (Uehara et al., 2010). In $DipM_{Ba}$, only two out of the four canonical catalytic residues are conserved (Figure S8), meaning that it is most probably inactive as an endopeptidase (Bochtler et al., 2004; Figueroa-Cuilan et al., 2021). Finding interacting partners of $DipM_{Ba}$ could help in deciphering its exact function in *B. abortus*. Unlike $DipM_{At}$ and CdlP, $DipM_{Ba}$ seems to be located only at the constriction site, and not at the growing pole (Figure 5) (Figueroa-Cuilan et al., 2021). In *C. crescentus*, DipM septal localization was shown to be dependent on its LysM domain, which is also present in $DipM_{Ba}$ (Moll et al., 2010). Additionally, it would be worth to investigate the function of other endopeptidases in *B. abortus* (Table S1) and in particular BAB1_1846, that is also predicted to be directly regulated by the cell division activator CtrA.

The CdlP lipoprotein is predicted to be a zinc-dependent M48 protease. CdlP is both localized at constriction sites and growing poles in *B. abortus*. CdlP displays homologs in several genera of Rhizobiales like *Agrobacterium*, *Sinorhizobium*, *Phyllobacterium*, *Mesorhizobium*, and *Bartonella*, suggesting that it could have co-evolved with unipolar growth. CdlP possesses a PG-binding LysM domain. The M48 peptidase domain of CdlP displays many homologs including BepA in *E. coli* (Daimon et al., 2017; Narita et al., 2013) and Oma1, a negative regulator of mitochondrial fusion in humans (Murata et al., 2020).

A common feature of CdlP, endopeptidases, and amidases in general is that all these enzymes depend on zinc as a cofactor, and histidine is most often the metal binding residue (Vermassen et al., 2019). The ability of histidine to complex metal has already been demonstrated (Nairn et al., 2016). It is tempting to speculate that our *hisB* mutants would have impaired metal homeostasis, which could in turn locally affect the activity of some key metalloenzymes involved in PG splitting, which probably includes CdlP and DipM but also most likely other metalloenzymes which have not yet been described in *B. abortus*. This hypothesis is supported by the fact that exposure to zinc triggers a chaining morphology in the parental strain (Figure S3). Moreover, the presence of the metal chelator EDTA significantly reduced chaining in the Δ*hisB* mutant (Figure S3).

Histidine metabolism has been already associated with filamentation phenotypes in *Escherichia coli* and *Salmonella enterica* serovar Typhimurium (Frandsen & D'Ari, 1993; Murray & Hartman, 1972). In those two bacterial species, division was inhibited when HisFH enzymes were overproduced, for reasons that remain unclear (Cano et al., 1998; Frandsen & D'Ari, 1993). Based on our results, we cannot exclude that the accumulation of IGP, the product of HisFH and the substrate of HisB (Figure S1), could be responsible for the phenotype of the *B. abortus hisB* mutants. However, in *Mycobacterium smegmatis*, histidine auxotroph mutants in almost the whole biosynthesis pathway genes exhibited a filamentation phenotype, all of which could be rescued by histidine supplementation, suggesting a link between cell division inhibition and histidine limitation in this particular case (de Wet et al., 2020).

Maintaining bacterial cell wall integrity during division is challenging. Characterizing the chaining phenotype of a *B. abortus* histidine auxotroph allowed us to identify two new metalloenzymes required for normal cell division. These proteins, DipM and CdlP, are conserved in alphaproteobacteria and even more distantly in chloroplast and mitochondria. A deeper investigation of the molecular mechanisms involved in PG hydrolysis during cell division is needed to understand how a mutation in an a priori unrelated metabolic pathway is able to affect this crucial and well controlled process, which is still largely underinvestigated in bacterial pathogens such as *B. abortus*.

4 | MATERIALS AND METHODS

4.1 | Bacterial strains, media, and strains construction

E. coli strains were grown in Luria-Bertani medium at 37°C. Derivatives of the *B. abortus* 544 Nal^R strain were cultivated in TSB-rich medium (3% Bacto Tryptic Soy Broth) at 37°C. Alternatively, the rich medium Heart Infusion Broth (HI) was used to grow *B. abortus*. Two defined media were also used for *B. abortus*, Plommet Erythritol (PE) (Plommet, 1991) composed of 7 g/L K_2HPO_4, 3 g/L KH_2PO_4, 0.1 g/L $Na_2S_2O_3$, 5 g/L NaCl, 0.2 mg/L nicotinic acid, 0.2 mg/L thiamine, 0.04 mg/L pantothenic acid, 0.01 g/L $MgSO_4$, 0.01 mg/L $MnSO_4$, 0.1 mg/L $FeSO_4$, 0.1 μg/L biotin and 2 g/L erythritol, and Gerhardt medium (Gerhardt & Wilson, 1948) composed of 30 g/L glycerol, 5 g/L lactate, 5 g/L glutamate, 10 g/L K_2HPO_4, 0.1 g/L $Na_2S_2O_3$, 7.5 g/L NaCl, 0.4 mg/L nicotinic acid, 0.2 mg/L thiamine, 0.2 mg/L pantothenic acid, 0.5 g/L $(NH_4)_2SO_4$, 0.01 g/L $MgSO_4$, 0.01 mg/L $MnSO_4$, 0.1 mg/L $FeSO_4$, 0.1 μg/L biotin. For the growth measurements in PE, the *B. abortus* strains were first grown overnight in TSB, next they were diluted to reach an exponential phase, then they were washed twice with PBS and diluted to reach an OD_{600nm} of 0.1 in PE (with or without 1 mM histidine). Antibiotic concentrations are the following: ampicillin, 100 μg/ ml; kanamycin, 10 or 50 μg/ml (10 μg/ml is chosen when kan^R marker is integrated in a chromosome of *B. abortus*); chloramphenicol, 20 μg/ml; nalidixic acid, 25 μg/ml; gentamicin, 50 μg/ml. The strains and plasmids used in this study are listed in Supporting Information, Tables S2 and S3, respectively. Details of their construction can be found in the Supporting Information text.

4.2 | CRISPR-interference

The CRISPRi plasmids (pJMP1039, pJMP1339, pJMP1356, and pJMP1339) were bought from Addgene (see Table S3) and were

a gift from Carol Gross, Jason Peters, and Oren Rosenberg. The pJMP1339t2 was constructed by Gibson Assembly (see SI appendix for more details). Single guide RNAs (sgRNAs) were designed with Benchling and chosen on the minus strand of the target promoter, then assembled on the *Bsa*I sites of the pJMP1339t$_2$ as detailed by the authors (Banta et al., 2020). Cloning steps until conjugation with *Brucella* were made as described by Banta and colleagues (Ducret et al., 2016). Primers that will be transcribed to sgRNA were hybridized by adding 1 µl of each primer (100 µM) to 5 µl of CutSmart 10X buffer (NEB) and scaled up to 50 µl with ddH_2O. The mix was then heated at 95 °C for 5 min and let cool down at room temperature (RT) for 15 min. Annealed oligos were diluted 40 times and 2 µl were used for ligation with the *Bsa*I restricted plasmid.

4.3 | HeLa cells culture and infection

HeLa cells (from the Centre d'Immunologie de Marseille-Luminy, Marseille, France) were cultivated at 37°C and in a 5% CO_2 atmosphere in DMEM (Invitrogen) supplemented with 10% fetal bovine serum (Gibco), 0.1 g/L non-essential amino acids, and 0.1 g/L sodium pyruvate (Invitrogen). For the infections, HeLa cells were seeded in 24-well plates (on coverslips for immunolabeling) at a concentration of 6.10^4 cells/ml. On the day of the infection, an overnight culture of *B. abortus* was diluted in DMEM to reach a MOI (multiplicity of infection) of 300. Bacteria were added to HeLa cells and the 24-well plates were centrifuged at 400 *g* for 10 min at RT. Cells were then incubated at 37°C in a 5% CO_2 atmosphere for 1 h. Cells were washed twice in PBS and fresh medium supplemented with 50 µg/ml gentamicin was added to kill extracellular bacteria. For CFU counts, at the different time points (2 h, 5 h, 24 h, and 48 h after infection) cells were washed twice in PBS, and then lysed with PBS with 0.1% Triton X-100 for 10 min at RT. Dilutions were then spotted (20 µl) onto TSB agar, incubated at 37 °C, and colony-forming units were counted. The CFU number was calculated per ml of lysate (0.5 ml per well). When indicated, 10 mM histidine was added in the medium at the beginning of the infection.

4.4 | Immunolabeling of infected HeLa cells

Cells were washed three times with PBS, then fixed in 2% paraformaldehyde (PFA) for 20 min at RT and permeabilized in PBS 0.1% Triton X-100 (Prolabo) for 10 min. Primary and secondary antibodies were diluted in PBS containing 0.1% Triton X-100 and 3% bovine serum albumin (BSA, Sigma-Aldrich). The immunodetection of intracellular *B. abortus* was made with a A76-12G12 monoclonal antibody (Cloeckaert et al., 1992) (hybridoma culture supernatant not diluted) followed by goat anti-mouse secondary antibodies coupled to Alexa 488 or Texas red diluted 500 times (Sigma Aldrich). The coverslips were washed three times with PBS, then once with ddH_2O and mounted with Mowiol (Sigma).

4.5 | PG isolation for morphology analysis

An overnight culture of around 7.5 ml of *B. abortus* in HI medium was pelleted (4600 *g*, 2.5 min), resuspended in 1 ml PBS, and then inactivated for 1 h at 80°C. Cells were pelleted again for 10 min at 10,000 *g* and then heated for 3 h in 1 ml 5% SDS at 95°C. Cells were washed three times with PBS and then 2 µl were dropped on an agarose pad (1% PBS agarose) for microscopy.

4.6 | eFluor and PG labeling

Exponential phase bacteria were washed (4600 *g*, 2.5 min) twice with PBS resuspended in eBioscience™ Cell Proliferation Dye eFluor™ 670 (eFluor, Invitrogen) at a final concentration of 5 µM in PBS. After 15 min of incubation at RT with shaking and protected from light, bacteria were washed twice and resuspended either in DMEM or in HI, for the generation of chains inside host cells or in growth medium, respectively. For PG labeling, after 5 h of growth in HI, bacteria were short pulse labeled for 5 min with 7-hydroxycoumarin 3-carboxylic acid coupled to 3-amino-D-alanine (HADA) (Uehara et al., 2009) at a final concentration of 500 µM in HI, protected from the light. Cells were pelleted and resuspended in 70% ice cold ethanol. After 15 min of incubation on ice, cells are washed 3 times with PBS before being observed by fluorescence microscopy.

4.7 | Microscopy and analysis

Bacteria were observed on 1% agarose PBS pad with an inverted microscope Nikon Eclipse Ti2 (oil objective 100x, CFI plan Apo Lambda DM 100XH 1.45/0.13 mm). Pictures were acquired with an Orca Flash 4.0 V3 (Hamamatsu). All images were analyzed with MicrobeJ, a plug-in of ImageJ (Ducret et al., 2016; Schneider et al., 2012). For length quantification, only isolated bacteria were analyzed and disrupted bacteria as well as cell aggregates were excluded from the analysis. For strains labeled with eFluor, only bacteria possessing a unique polar eFluor signal were used to construct a demographic representation.

AUTHOR CONTRIBUTIONS

Xavier De Bolle and Agnès Roba designed research. Agnès Roba performed all experiments, unless stated otherwise, Elodie Carlier made cellular infections and fluorescence microscopy, Pierre Godessart and Cerine Naili set up the CRISPRi applied to *B. abortus* and generated the depletion strains. Agnès Roba and Xavier De Bolle wrote the paper.

ACKNOWLEDGMENTS

We are grateful to Marty Roop and Jean-Jacques Letesson for their advices in the writing of this manuscript. We thank Stéphane Vincent and his team for the synthesis of HADA, Neeraj Dhar for advices regarding mNeonGreen, as well as Mathieu Waroquier, Françoise

Tilquin, and Aurélie Mayard for their technical assistance. This research has been funded by grants from the *Fonds de la Recherche Scientifique-Fonds National de la Recherche Scientifique* (FRS-FNRS, http://www.fnrs.be) (PDR Brucell-cycle T.0060.15, and PDR Single cell analysis of *Brucella* growth T.0058.20) to X. De Bolle. The work was also supported by a grant from Actions de Recherche Concertée 17/22-087 from the *Fédération Wallonie-Bruxelles* of Belgium. Agnès Roba and Pierre Godessart hold a PhD fellowship from FRS-FNRS (Aspirant and FRIA, respectively). We thank the University of Namur for logistic support.

CONFLICT OF INTEREST

The authors declare no conflict of interest.

DATA AVAILABILITY STATEMENT

Data available on request from the authors.

ORCID

Xavier De Bolle https://orcid.org/0000-0002-3845-3043

REFERENCES

Banta, A.B., Enright, A.L., Siletti, C. & Peters, J.M. (2020) A high-efficacy CRISPR interference system for gene function discovery in *Zymomonas mobilis*. *Applied and Environmental Microbiology*, *86*, e01621-20.

Batut, J., Andersson, S.G. & O'Callaghan, D. (2004) The evolution of chronic infection strategies in the alpha-proteobacteria. *Nature Reviews. Microbiology*, *2*, 933–945.

Bochtler, M., Odintsov, S.G., Marcyjaniak, M. & Sabala, I. (2004) Similar active sites in lysostaphins and D-Ala-D-Ala metallopeptidases. *Protein Science*, *13*, 854–861.

Brown, P.J., de Pedro, M.A., Kysela, D.T., van der Henst, C., Kim, J., De Bolle, X. et al. (2012) Polar growth in the alphaproteobacterial order rhizobiales. *Proceedings of the National Academy of Sciences of the United States of America*, *109*, 1697–1701.

Cano, D.A., Mouslim, C., Ayala, J.A., García-del Portillo, F. & Casadesús, J. (1998) Cell division inhibition in *Salmonella typhimurium* histidine-constitutive strains an ftsI-like defect in the presence of wild-type penicillin-binding protein 3 levels. *Journal of Bacteriology*, *180*, 5231–5234.

Celli, J., de Chastellier, C., Franchini, D.M., Pizarro-Cerda, J., Moreno, E. & Gorvel, J.P. (2003) *Brucella* evades macrophage killing via VirB-dependent sustained interactions with the endoplasmic reticulum. *The Journal of Experimental Medicine*, *198*, 545–556.

Cloeckaert, A., Jacques, I., de Wergifosse, P., Dubray, G. & Limet, J.N. (1992) Protection against *Brucella melitensis* or *Brucella abortus* in mice with immunoglobulin G (IgG), IgA, and IgM monoclonal antibodies specific for a common epitope shared by the *Brucella* A and M smooth lipopolysaccharides. *Infection and Immunity*, *60*, 312–315.

Daimon, Y., Iwama-Masui, C., Tanaka, Y., Shiota, T., Suzuki, T., Miyazaki, R. et al. (2017) The TPR domain of BepA is required for productive interaction with substrate proteins and the beta-barrel assembly machinery complex. *Molecular Microbiology*, *106*, 760–776.

de Wet, T.J., Winkler, K.R., Mhlanga, M., Mizrahi, V. & Warner, D.F. (2020) Arrayed CRISPRi and quantitative imaging describe the morphotypic landscape of essential mycobacterial genes. *eLife*, *9*, e60083.

Ducret, A., Quardokus, E.M. & Brun, Y.V. (2016) MicrobeJ, a tool for high throughput bacterial cell detection and quantitative analysis. *Nature Microbiology*, *1*, 16077.

Eberhardt, C., Kuerschner, L. & Weiss, D.S. (2003) Probing the catalytic activity of a cell division-specific transpeptidase in vivo with beta-lactams. *Journal of Bacteriology*, *185*, 3726–3734.

Figueroa-Cuilan, W.M., Randich, A.M., Dunn, C.M., Santiago-Collazo, G., Yowell, A. & Brown, P.J.B. (2021) Diversification of LytM protein functions in polar elongation and cell division of *Agrobacterium tumefaciens*. *Frontiers in Microbiology*, *12*, 729307.

Francis, N., Poncin, K., Fioravanti, A., Vassen, V., Willemart, K., Ong, T.A. et al. (2017) CtrA controls cell division and outer membrane composition of the pathogen *Brucella abortus*. *Molecular Microbiology*, *103*, 780–797.

Frandsen, N. & D'Ari, R. (1993) Excess histidine enzymes cause AICAR-independent filamentation in *Escherichia coli*. *Molecular & General Genetics*, *240*, 348–350.

Gerhardt, P. & Wilson, J.B. (1948) The nutrition of Brucellae: growth in simple chemically defined media. *Journal of Bacteriology*, *56*, 17–24.

Heidrich, C., Ursinus, A., Berger, J., Schwarz, H. & Holtje, J.V. (2002) Effects of multiple deletions of murein hydrolases on viability, septum cleavage, and sensitivity to large toxic molecules in *Escherichia coli*. *Journal of Bacteriology*, *184*, 6093–6099.

Kuru, E., Hughes, H.V., Brown, P.J., Hall, E., Tekkam, S., Cava, F. et al. (2012) In situ probing of newly synthesized peptidoglycan in live bacteria with fluorescent D-amino acids. *Angewandte Chemie (International Ed. in English)*, *51*, 12519–12523.

Latch, J.N. & Margolin, W. (1997) Generation of buds, swellings, and branches instead of filaments after blocking the cell cycle of *Rhizobium meliloti*. *Journal of Bacteriology*, *179*, 2373–2381.

Miyagishima, S.Y., Kabeya, Y., Sugita, C., Sugita, M. & Fujiwara, T. (2014) DipM is required for peptidoglycan hydrolysis during chloroplast division. *BMC Plant Biology*, *14*, 57.

Moll, A., Schlimpert, S., Briegel, A., Jensen, G.J. & Thanbichler, M. (2010) DipM, a new factor required for peptidoglycan remodelling during cell division in *Caulobacter crescentus*. *Molecular Microbiology*, *77*, 90–107.

Murata, D., Yamada, T., Tokuyama, T., Arai, K., Quirós, P.M., López-Otín, C. et al. (2020) Mitochondrial safeguard: a stress response that offsets extreme fusion and protects respiratory function via flickering-induced Oma1 activation. *The EMBO Journal*, *39*, e105074.

Murray, M.L. & Hartman, P.E. (1972) Overproduction of hisH and hisF gene products leads to inhibition of cell division in *Salmonella*. *Canadian Journal of Microbiology*, *18*, 671–681.

Nairn, B.L., Lonergan, Z.R., Wang, J., Braymer, J.J., Zhang, Y., Calcutt, M.W. et al. (2016) The response of *Acinetobacter baumannii* to zinc starvation. *Cell Host & Microbe*, *19*, 826–836.

Narita, S., Masui, C., Suzuki, T., Dohmae, N. & Akiyama, Y. (2013) Protease homolog BepA (YfgC) promotes assembly and degradation of beta-barrel membrane proteins in *Escherichia coli*. *Proceedings of the National Academy of Sciences of the United States of America*, *110*, E3612–E3621.

Pappas, G., Papadimitriou, P., Akritidis, N., Christou, L. & Tsianos, E.V. (2006) The new global map of human brucellosis. *The Lancet Infectious Diseases*, *6*, 91–99.

Plommet, M. (1991) Minimal requirements for growth of *Brucella suis* and other *Brucella* species. *Zentralblatt für Bakteriologie*, *275*, 436–450.

Schneider, C.A., Rasband, W.S. & Eliceiri, K.W. (2012) NIH Image to ImageJ: 25 years of image analysis. *Nature Methods*, *9*, 671–675.

Sharma, A.K., Kumar, S., H., K., Dhakan, D.B. & Sharma, V.K. (2016) Prediction of peptidoglycan hydrolases- a new class of antibacterial proteins. *BMC Genomics*, *17*, 411.

Starr, T., Ng, T.W., Wehrly, T.D., Knodler, L.A. & Celli, J. (2008) *Brucella* intracellular replication requires trafficking through the late endosomal/lysosomal compartment. *Traffic*, *9*, 678–694.

Sternon, J.F., Godessart, P., Gonçalves de Freitas, R., van der Henst, M., Poncin, K., Francis, N. et al. (2018) Transposon sequencing of *Brucella abortus* uncovers essential genes for growth in vitro and inside macrophages. *Infection and Immunity*, *86*, e00312-18.

Uehara, T., Dinh, T. & Bernhardt, T.G. (2009) LytM-domain factors are required for daughter cell separation and rapid ampicillin-induced lysis in *Escherichia coli*. *Journal of Bacteriology*, *191*, 5094–5107.

Uehara, T., Parzych, K.R., Dinh, T. & Bernhardt, T.G. (2010) Daughter cell separation is controlled by cytokinetic ring-activated cell wall hydrolysis. *The EMBO Journal*, *29*, 1412–1422.

Vassen, V., Valotteau, C., Feuillie, C., Formosa-Dague, C., Dufrêne, Y.F. & De Bolle, X. (2019) Localized incorporation of outer membrane components in the pathogen *Brucella abortus*. *The EMBO Journal*, *38*, e100323.

Vermassen, A., Leroy, S., Talon, R., Provot, C., Popowska, M. & Desvaux, M. (2019) Cell wall hydrolases in bacteria: insight on the diversity of cell wall amidases, glycosidases and peptidases toward peptidoglycan. *Frontiers in Microbiology*, *10*, 331.

Whatmore, A.M. & Foster, J.T. (2021) Emerging diversity and ongoing expansion of the genus *Brucella*. *Infection, Genetics and Evolution*, *92*, 104865.

Yakhnina, A.A. & Bernhardt, T.G. (2020) The Tol-Pal system is required for peptidoglycan-cleaving enzymes to complete bacterial cell division. *Proceedings of the National Academy of Sciences of the United States of America*, *117*, 6777–6783.

SUPPORTING INFORMATION

Additional supporting information can be found online in the Supporting Information section at the end of this article.

How to cite this article: Roba, A., Carlier, E., Godessart, P., Naili, C. & De Bolle, X. (2022). Histidine auxotroph mutant is defective for cell separation and allows the identification of crucial factors for cell division in *Brucella abortus*. *Molecular Microbiology*, *00*, 1–10. https://doi.org/10.1111/mmi.14956